Supplementary Information

A splicing isoform of PD-1 promotes tumor progression as a potential immune checkpoint

Xuetong Wang[1,2,3], Tongfeng Liu[3,4], Yifei Li[3,5], Ao Ding[3,5], Chang Zhang[3,6], Yinmin Gu[3], Xujie Zhao[3], Shuwen Cheng[3,7], Tianyou Cheng[8], Songzhe Wu[3], Liqiang Duan[8], Jihang Zhang[3,4], Rong Yin[9], Man Shang[10], Shan Gao[1,2,3]✉

[1] School of Biomedical Engineering (Suzhou), Division of Life Sciences and Medicine, University of Science and Technology of China, Hefei 230000, China; [2] Suzhou Institute of Biomedical Engineering and Technology, Chinese Academy of Science, Suzhou 215163, China; [3] Zhongda Hospital, School of Life Sciences and Technology, Advanced Institute for Life and Health, Southeast University, Nanjing 210096, China; [4] Medical School of Guizhou University, Guiyang 550025, China; [5] School of Pharmacy, Nanjing University of Chinese Medicine, Nanjing 210023, China; [6] Department of medical oncology, The Key Laboratory of Advanced Interdisciplinary Studies Center, State Key Laboratory of Respiratory Disease, The First Affiliated Hospital of Guangzhou Medical University, Guangzhou Medical University, Guangdong 510120, China; [7] Medical School of Nanjing University, Nanjing 210046, China; [8] Shanxi Academy of Advanced Research and Innovation, Taiyuan 030032, China; [9] Nanjing Medical University Affiliated Cancer Hospital, Nanjing 210096, China; [10] Nanjing Women and Children's Healthcare Institute, Women' s Hospital of Nanjing Medical University (Nanjing Women and Children' s Healthcare Hospital), Nanjing 210096, China. ✉email: gaos@sibet.ac.cn

Supplementary Figures

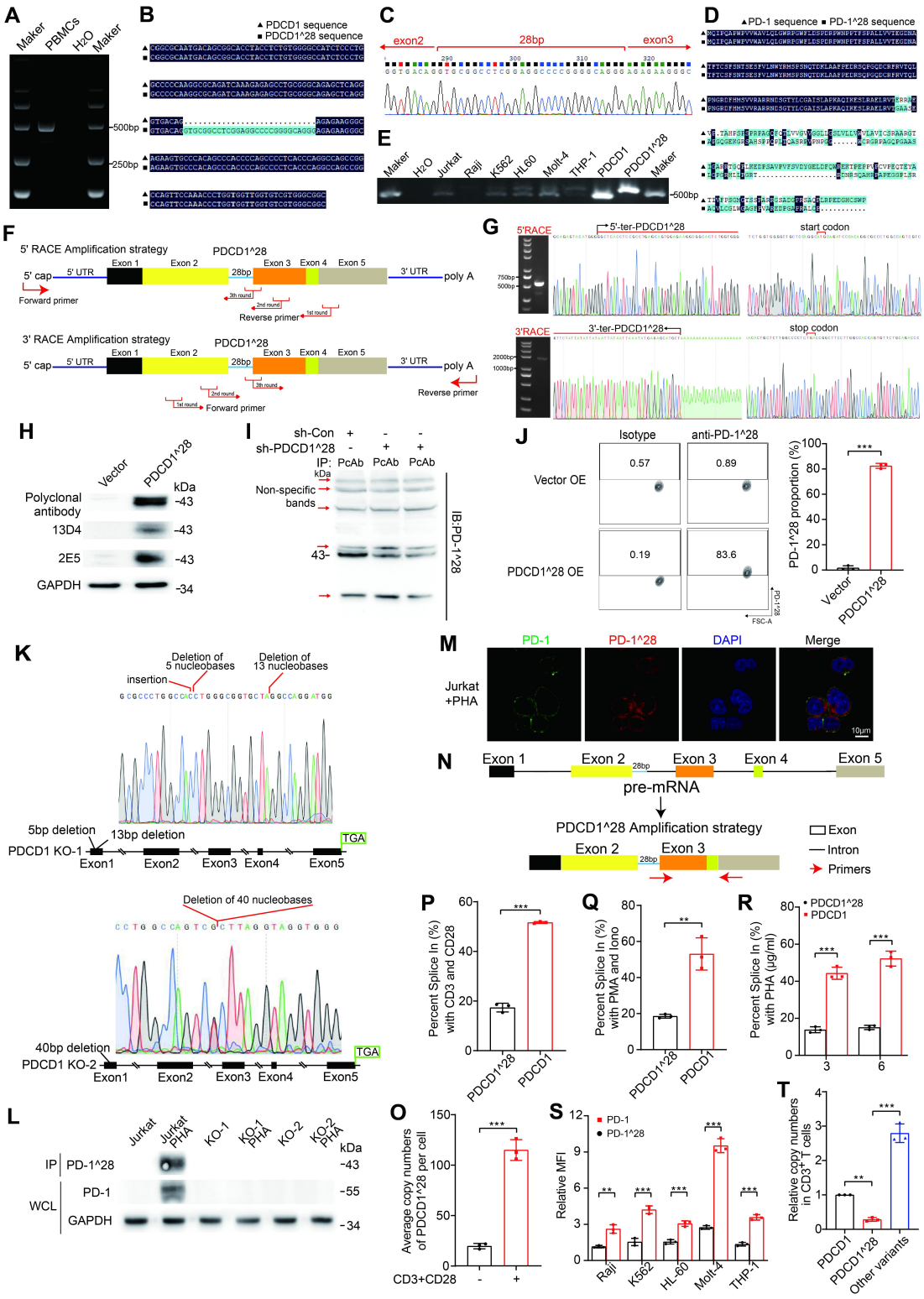

Fig. S1 | The identification and characterization of PD-1^28. Related to Figure 1. (A and C) *PDCD1* PCR products (A) and DNA sequence analysis of *PDCD1^28* clone (C) amplified in cDNA of a healthy human PBMCs. Lane H_2O

is a negative control. (B and D) Comparison of nucleotide sequences between *PDCD1* and *PDCD1^28* (B) and amino acid sequences between PD-1 and PD-1^28 (D). (E) *PDCD1* and *PDCD1^28* PCR products were amplified in cDNA of various human leukaemia cell lines. Lanes of *PDCD1* and *PDCD1^28* are positive controls. Lane H_2O is a negative control. (F) The schematic diagram for 5'- (top) and 3'- (bottom) RACE amplification of *PDCD1^28*. (G) The 5'- (top) and 3'- (bottom) RACE analysis of *PDCD1^28* sequence. Sequence of PCR products reveal the boundaries between universal anchor primers and *PDCD1^28* sequences. Arrows indicate the transcription direction. Terminal (ter). (H and J) The specificity of PD-1^28 antibodies were verified by immunoblot analysis of the indicated proteins (H) and monoclonal antibody verified by flow cytometry of HEK293T cells transfected with the indicated plasmids (J) (n = 3 biologically independent experiments). (I) Immunoblot analysis of immunoprecipitation of endogenous PD-1^28 in Jurkat cells transfected with the indicated plasmids. Non-specific bands were indicated by red arrows. (K) DNA sequence analyses (top) and the schematic gene structure (bottom) of *PDCD1* KO-1 and KO-2 Jurkat cells. (L) Immunoblot analysis for KO efficiency of PD-1^28 and PD-1in *PDCD1* KO-1 and KO-2 Jurkat cells. (M) Representative confocal images of endogenous PD-1^28 (red) and PD-1 (green) in Jurkat cells activated by PHA. The nuclei (blue) were stained with DAPI. Scale bars, 10 μm. (N) The schematic diagram for PCR-based specific amplification of *PDCD1^28*. (O) The copy numbers of *PDCD1^28* in Jurkat cells before and after stimulation with antibodies of CD3 and CD28 (n = 3 biologically independent experiments). (P-R) PSI values for *PDCD1^28* and *PDCD1* splicing event in Jurkat cells stimulated by CD3 and CD28 (P), PMA and Ionomycin (Q) or PHA (R) (n = 3 biologically independent experiments). (S) FACS analysis for PD-1^28 and PD-1 in various human leukemia cell lines and quantified as the MFI (n = 3 biologically independent experiments). (T) The copy numbers of *PDCD1*, *PDCD1^28*, and other variants in $CD3^+$ T cells from PBMCs of 3 healthy human donors. The copy

numbers were normalized to *PDCD1.* Data represent the mean ± SD. Statistical significance was determined by two-tailed unpaired Student's *t*-test (J, O-S) or one-way ANOVA with Tukey post hoc test (T). *$p < 0.05$, **$p < 0.01$, ***$p < 0.001$. Source data, including exact *p*-values, are provided as a Source Data file.

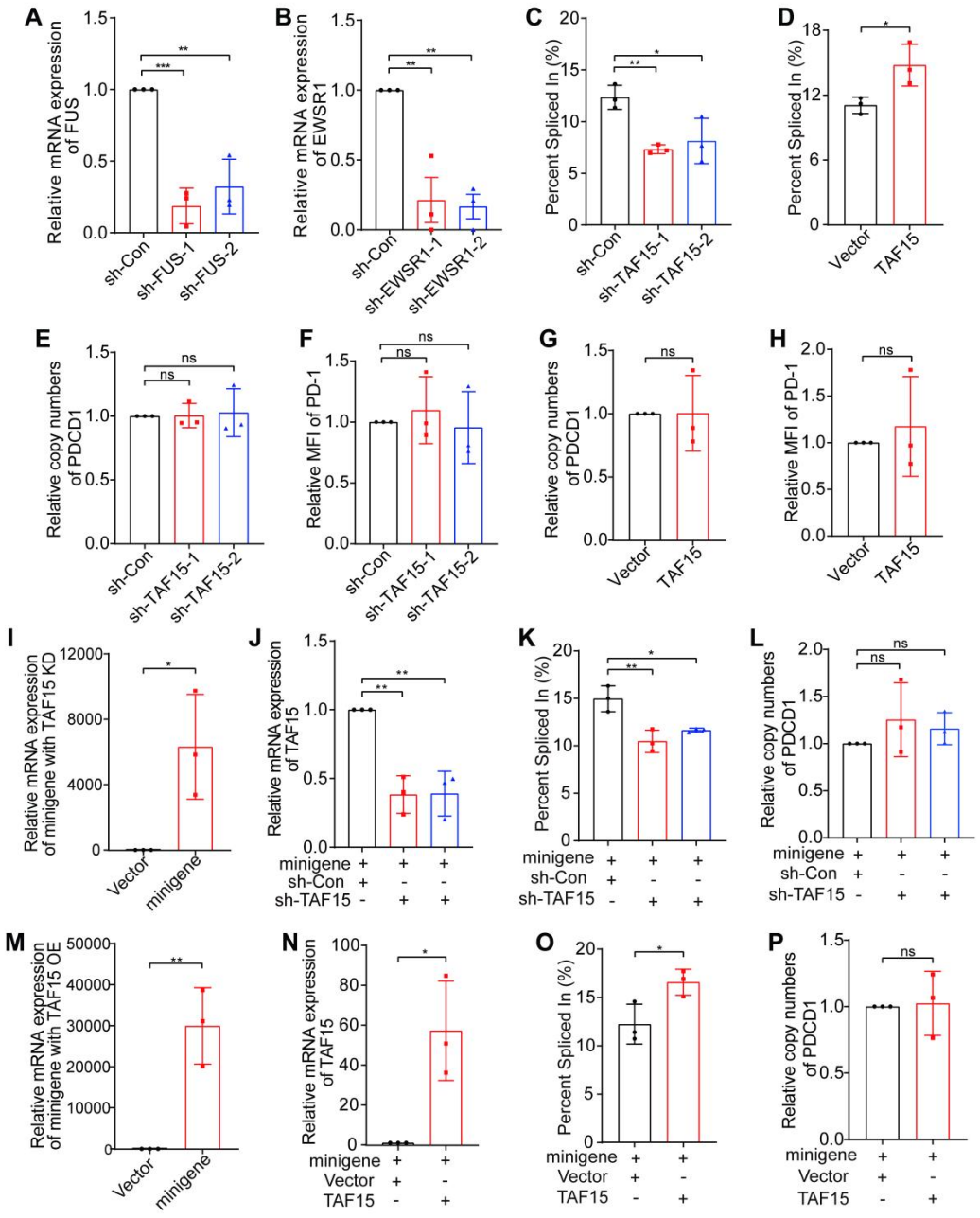

Fig. S2 | Splicing of *PDCD1^28* is regulated by TAF15. Related to Figure 2. (A and B) qRT-PCR analysis for *FUS* (A) or *EWSR1* (B) in Jurkat cells transfected with the indicated shRNAs (n = 3 biologically independent experiments). (C and D) PSI values for *PDCD1^28* splicing event in *TAF15* KD (C) or OE (D) Jurkat cells (n = 3 biologically independent experiments). (E-H) The copy numbers of *PDCD1* (E and G) or quantitation of PD-1 levels as MFI (F and H) in *TAF15* KD (E and F) or OE (G and H) Jurkat cells (n = 3 biologically independent experiments). The copy numbers were normalized to

the control group. (I and M) qRT-PCR analysis for *minigene* with *TAF15* KD (I) or OE (M) in HEK293T cells (n = 3 biologically independent experiments). (J and N) qRT-PCR analysis for KD (J) or OE (N) of *TAF15* in *minigene* OE HEK293T cells transfected with the indicated plasmids (n = 3 biologically independent experiments). (K and O) PSI values for *PDCD1^28* splicing event in *minigene* OE HEK293T cells with *TAF15* KD (K) or OE (O) (n = 3 biologically independent experiments). (L and P) The copy numbers of *PDCD1* in *minigene* OE HEK293T cells with *TAF15* KD (L) or OE (P) (n = 3 biologically independent experiments). The copy numbers were normalized to the control group. Data represent the mean ± SD (A and C-P) or SEM (B). Statistical significance was determined by one-way ANOVA with Dunnett post hoc test (A-C, E-F and J-L) or two-tailed unpaired Student's *t*-test (D, G-I and M-P). **p* < 0.05, ***p* < 0.01, ****p* < 0.001. Source data, including exact *p*-values, are provided as a Source Data file.

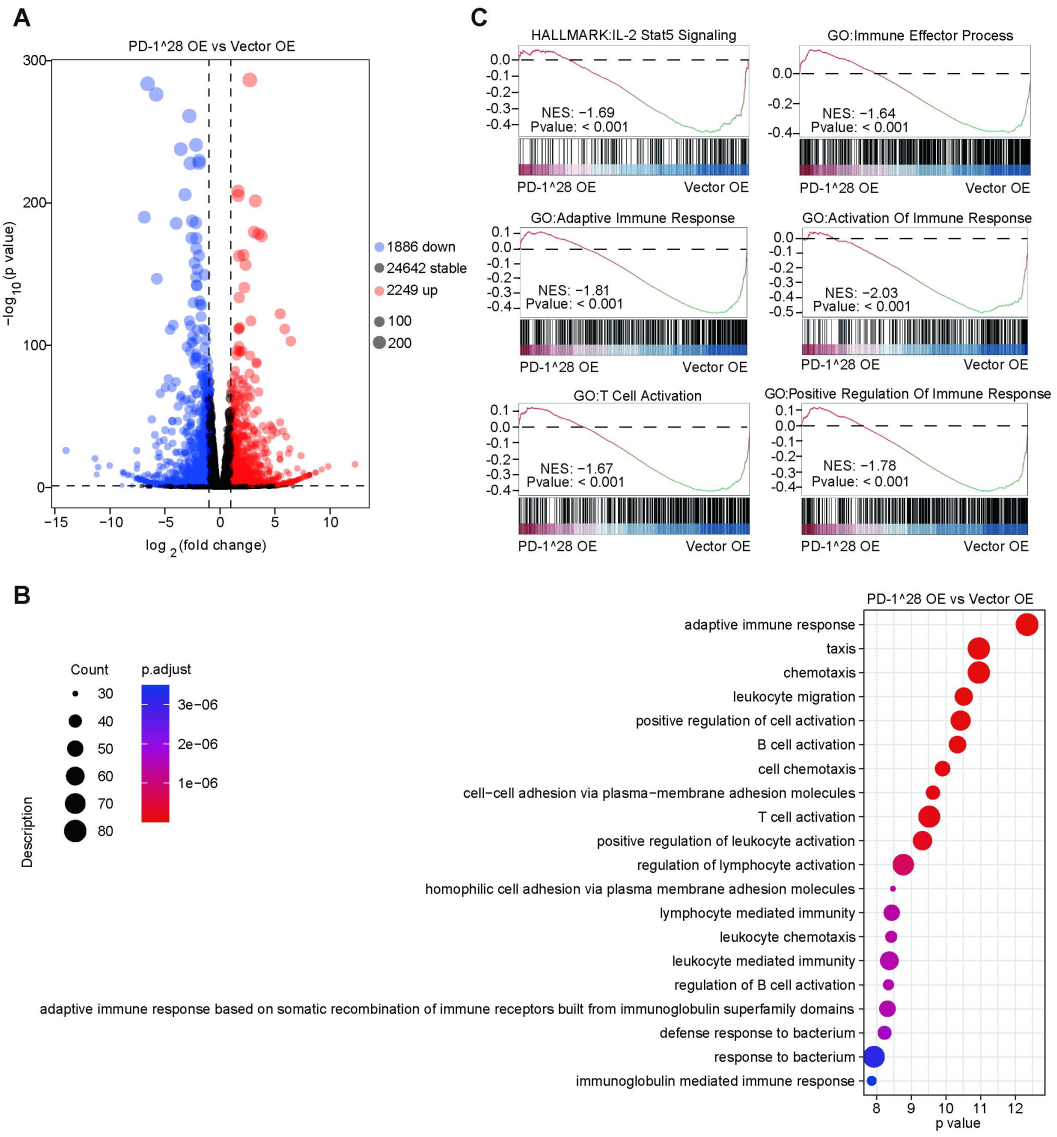

Fig. S3 | RNA-seq analysis of *PDCD1^28* OE cells. Related to Figure 3. (A) Volcano plot of the downregulation of 1886 genes (blue) and upregulation of 2249 genes (red) between *PDCD1^28* OE and control *PDCD1* KO-1 Jurkat cells. (B) Top 20 enriched GO terms showing the significantly enriched pathways from the down-regulated genes from (A). The color intensity indicates the *p* values. The size of the circle represents the number of enriched proteins in the term. (C) GSEA analysis showing the enrichment of “IL2 Stat5 Signaling”, “Immune Effector Process”, “Adaptive Immune Reponse”, “Activation Of Immune Response”, “T Cell Activation” and “Positive Regulation Of Immune Response” between *PDCD1^28* OE and control *PDCD1* KO-1 Jurkat cells.

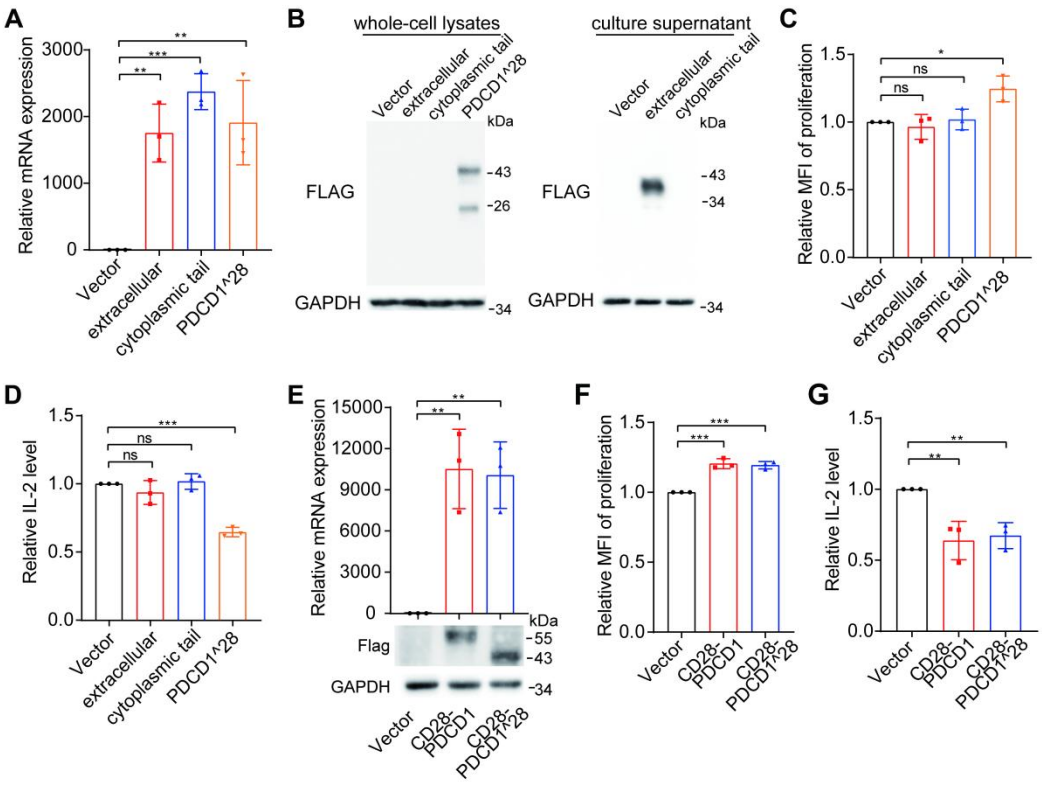

Fig. S4 | PD-1^28 exerts immunosuppressive function in T cells. Related to Figure 3. (A and E) qRT-PCR analysis for extracellular domain, cytoplasmic tail or *PDCD1^28* (A) and either *CD28-PDCD1* or *CD28-PDCD1^28* (E, top), and immunoblot analysis for the indicated proteins (E, bottom) in KO-1 cells transfected with the indicated plasmids (n = 3 biologically independent experiments). (B) Immunoblot analysis for the indicated proteins in the whole-cell lysates and the culture supernatant. (C and F) CFSE assay assessing the relative proliferation of KO-1 Jurkat cells with OE of extracellular domain, cytoplasmic tail or *PDCD1^28* (C), and either *CD28-PDCD1* or *CD28-PDCD1^28* (F) (n = 3 biologically independent experiments). (D and G) ELISA assessing the relative IL-2 production of KO-1 Jurkat cells with OE of extracellular domain, cytoplasmic tail or *PDCD1^28* (D), and either *CD28-PDCD1* or *CD28-PDCD1^28* (G) (n = 3 biologically independent experiments). Data represent the mean ± SD. Statistical significance was determined by one-way ANOVA with Dunnett post hoc test (A and C-G). *p < 0.05, **p < 0.01, ***p < 0.001. Source data, including exact *p*-values, are provided as a Source Data file.

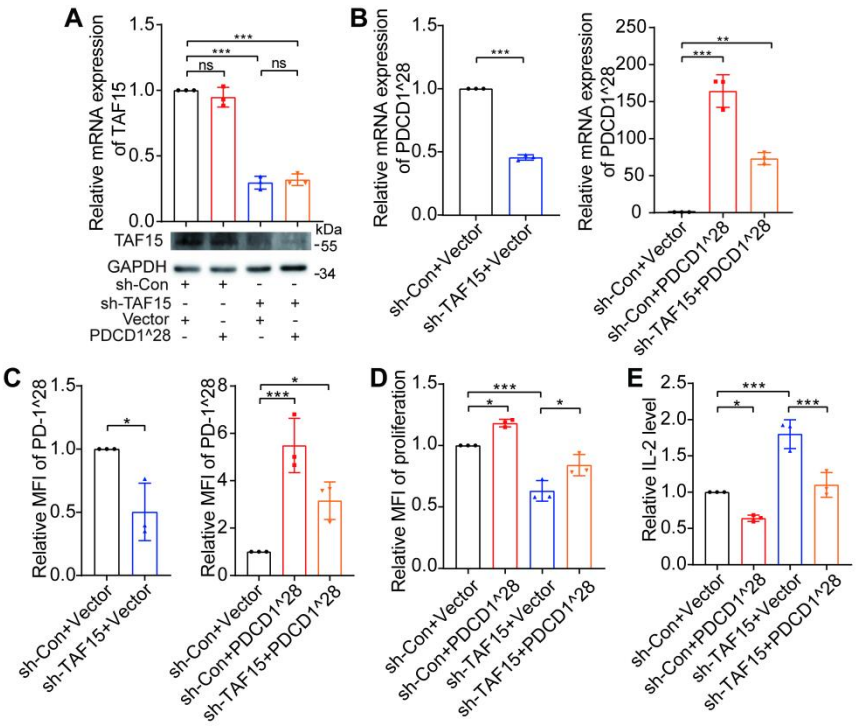

Fig. S5 | The regulation of the alternative splicing for *PDCD1^28* related to the immune function. Related to Figure 3. (A) qRT-PCR analysis for *TAF15* (top) and immunoblot analysis for the indicated proteins (bottom) in Jurkat cells transfected with the indicated plasmids (n = 3 biologically independent experiments). (B and C) qRT-PCR analysis for *PDCD1^28* (B), and FACS analysis for PD-1^28 protein levels, quantified as MFI (C) (n = 3 biologically independent experiments). (D and E) CFSE assay assessing the relative proliferation (D), and ELISA assessing the relative IL-2 production (E) (n = 3 biologically independent experiments). Data represent the mean ± SD. Statistical significance was determined by one-way ANOVA with Tukey (A, D, and E) or Dunnett (B and C, right) post hoc test or two-tailed unpaired Student's *t*-test (B and C, left). *p < 0.05, **p < 0.01, ***p < 0.001. Source data, including exact *p*-values, are provided as a Source Data file.

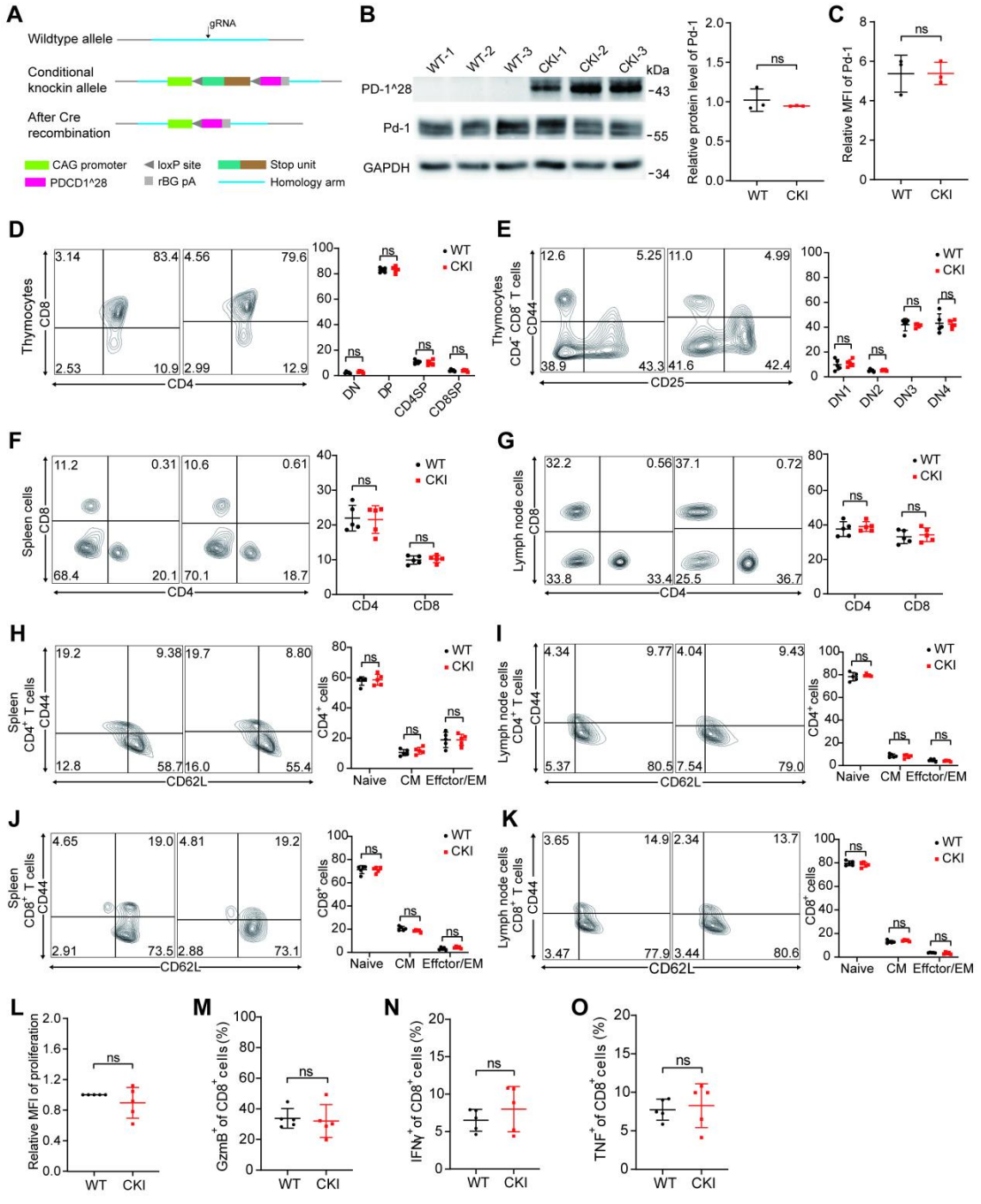

Fig. S6 | *PDCD1^28* knockin does not affect thymocyte development and peripheral T cell homeostasis. Related to Figure 6. (A) The construction strategy of *PDCD1^28*^{CKI} mice. (B) Immunoblot analysis for knock-in efficiency of PD-1^28 and Pd-1 of wild-type and *PDCD1^28*^{CKI} mice (left), and quantification results of Pd-1 (right) (n = 3 mice per group, female, age of 6-8 weeks). (C) FACS analysis for Pd-1 and quantified as the MFI (n = 3 mice per group, female, age of 6-8 weeks). (D-K) FACS analysis of thymocytes,

peripheral T cells isolated from spleen and lymph nodes of wild-type and *PDCD1^28^{CKI}* mice (n = 5). Left, representative flow cytometry profiles. Right, statistical analyses. (D) Percentages of $CD4^{-}CD8^{-}$ double-negative (DN), $CD4^{+}CD8^{+}$ double-positive (DP), $CD4^{+}$ single-positive (CD4SP) and $CD8^{+}$ single-positive (CD8SP) cells out of the total number of thymocytes from wild-type and *PDCD1^28^{CKI}* mice. (E) Percentages of $CD44^{+}$ single-positive (DN1), $CD44^{+}CD25^{+}$ double-positive (DN2), $CD25^{+}$ single-positive (DN3) and $CD44^{-}CD25^{-}$double-negative (DN4) cells in $CD4^{-}CD8^{-}$ cells from panel D. (F and G) Percentages of $CD4^{+}$ and $CD8^{+}$ T cells in spleen (F) and lymph nodes (G) of wild-type and *PDCD1^28^{CKI}* mice. (H-K) Percentages of naive ($CD44^{low}$ $CD62L^{high}$), central memory ($CD44^{high}$ $CD62L^{high}$; CM) and effector/effector memory ($CD44^{high}$ $CD62L^{low}$, effector/EM) $CD4^{+}$ and $CD8^{+}$ T cells in spleen (H and J) and lymph nodes (I and K) of wild-type and *PDCD1^28^{CKI}* mice. (L-O) Naive $CD8^{+}$ T cells isolated from wild-type and *PDCD1^28^{CKI}* mice were stimulated with anti-CD3 and anti-CD28 antibodies. Proliferation of wild-type or *PDCD1^28^{CKI}* $CD8^{+}$ T cells measured by CFSE (L). Cytokine production of wild-type or *PDCD1^28^{CKI}* $CD8^{+}$ T cells (M-O). Data represent the mean ± SD. Statistical significance was determined by two-tailed unpaired Student's *t*-test (B-O). $*p < 0.05$, $**p < 0.01$, $***p < 0.001$. Source data, including exact *p*-values, are provided as a Source Data file.

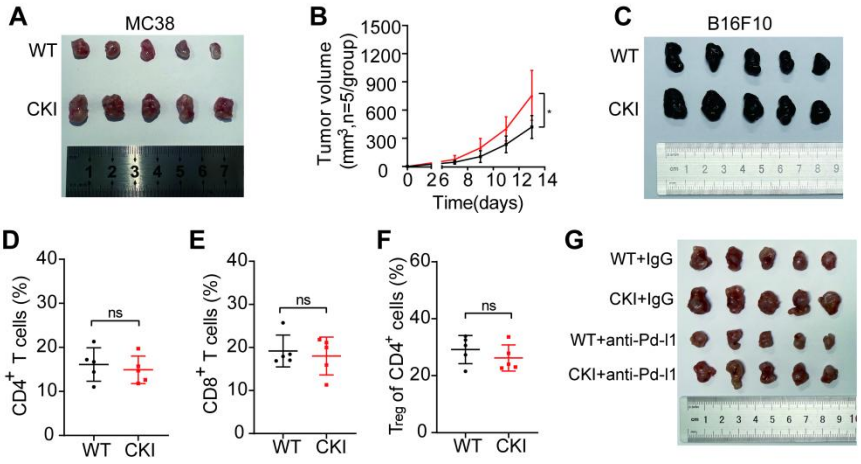

Fig. S7 | PD-1^28 regulates T cell anti-tumor immunity in MC38 colorectal carcinoma and B16F10 melanoma models. Related to Figure 6. (A) Tumor size in wild-type and *PDCD1^28^{CKI}* mice subcutaneously implanted with MC38 cells at the end point (n = 5). (B-F) B16F10 tumor progression and phenotype of tumor-infiltrating T cells were assessed in wild-type and *PDCD1^28^{CKI}* mice (n = 5). Tumor volume and tumor size (B and C). TILs were isolated and analyzed after transplantation. Frequencies of $CD4^+$ T cells (D), $CD8^+$ T cells (E), and T_{reg} cell population (F). (G) Tumor size in wild-type and *PDCD1^28^{CKI}* mice of anti-Pd-l1 therapy against MC38 colorectal carcinoma (n = 5). Data represent the mean ± SD. Statistical significance was determined by two-tailed unpaired Student's *t*-test (B and D-F).*$p < 0.05$, **$p < 0.01$, ***$p < 0.001$. Source data, including exact *p*-values, are provided as a Source Data file.

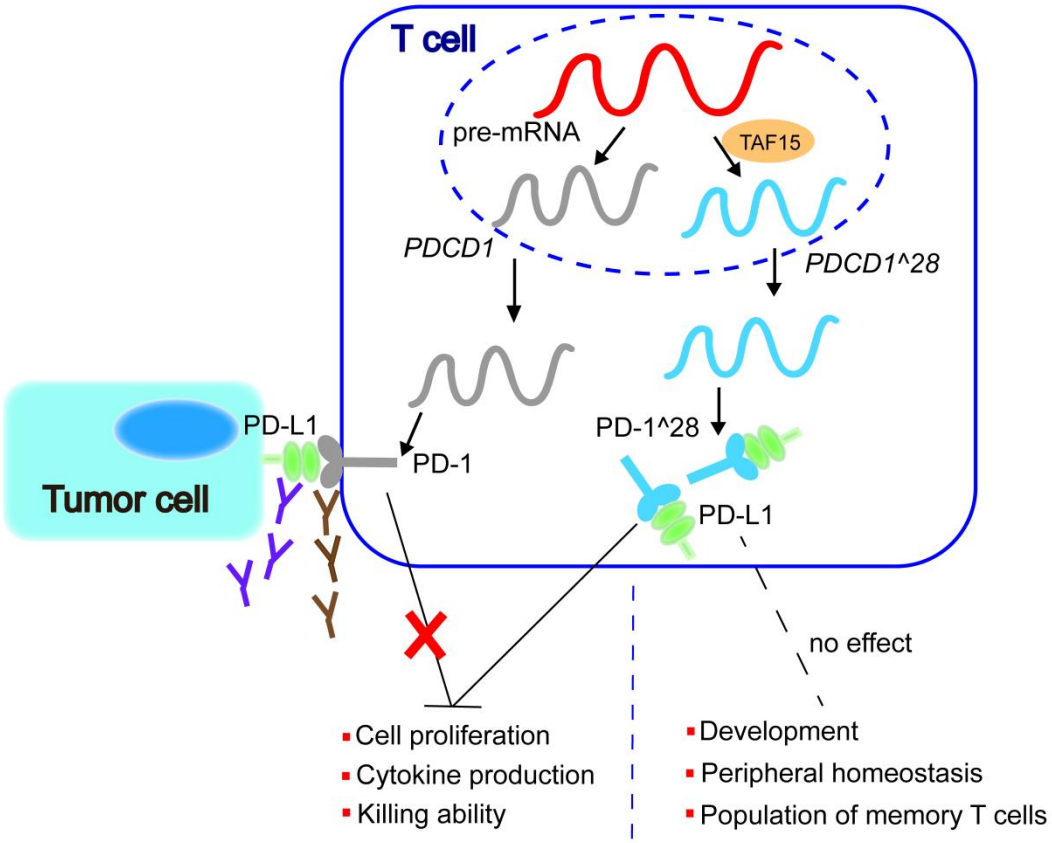

Fig. S8 | A schematic for regulation and function of PD-1^28. The RNA binding protein TAF15 specifically mediates the alternative splicing of pre-mRNA to *PDCD1^28* but does not affect the expression level of *PDCD1*. PD-1^28 expressed by T cells inhibits cell proliferation, cytokine production, and tumor cell killing, without affecting the development, peripheral homeostasis, and population of memory T cells. Antibodies targeting PD-1 (brown) or PD-L1 (purple) have no effects of PD-1^28 on T cells, thus leading to resistance to immune checkpoint blockade. We used Adobe Illustrator to produce Fig. S8.

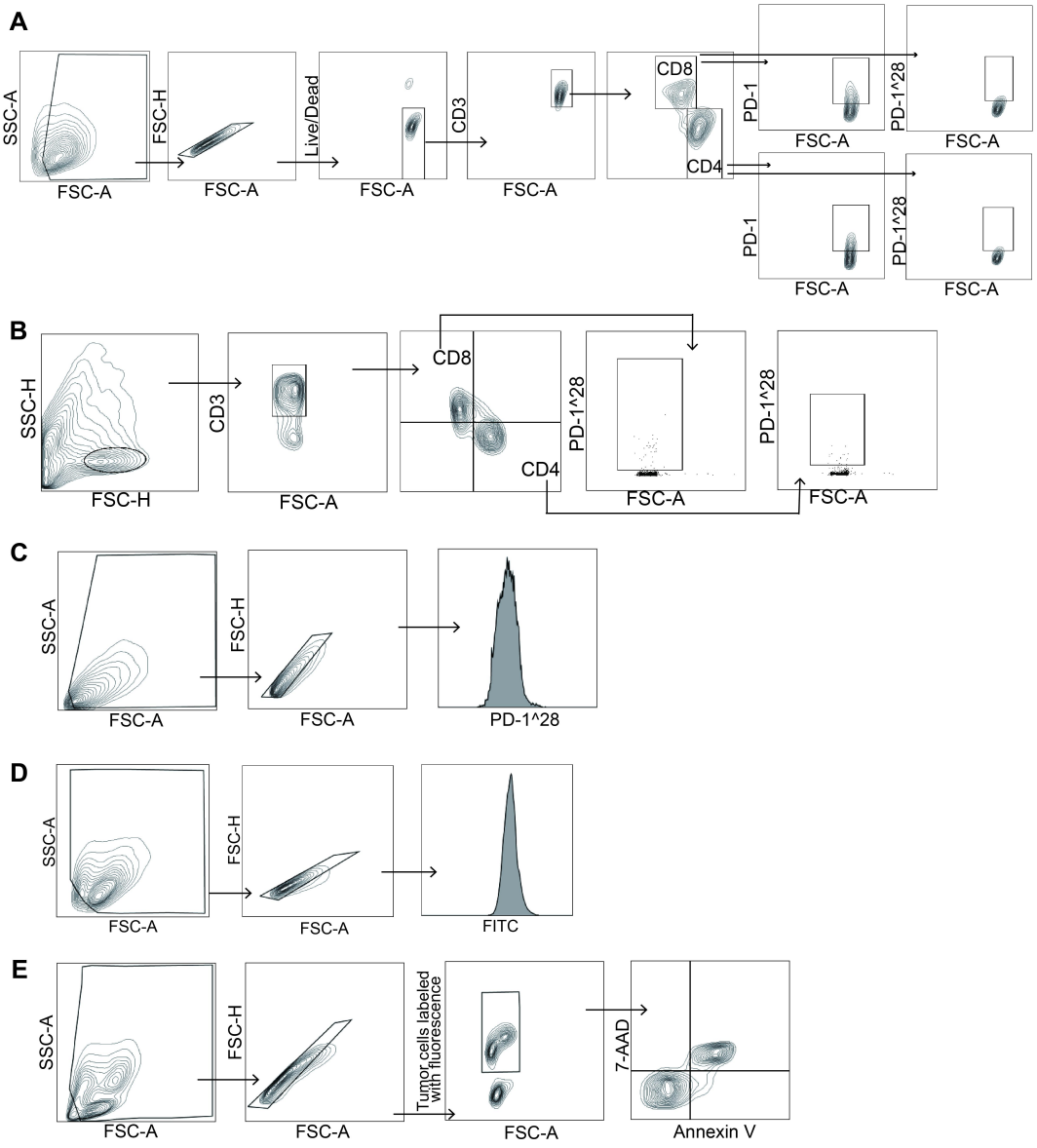

Fig. S9 | Gating strategies used for FACS. (A) Gating strategy to measure PD-1 and PD-1^28 proportion in CD4+ and CD8+ T cells from PBMCs presented on Fig. 1M. (B) Gating strategy to measure PD-1^28 proportion in CD4+ and CD8+ TILs presented on Fig. 1N. (C) Gating strategy to measure the MFI of PD-1^28 presented on Fig. 2K. (D) Gating strategy of proliferation assay presented on Fig. 3C. (E) Gating strategy to evaluate tumor cell killing presented on Fig. 3J. Isotype is used as a negative control.

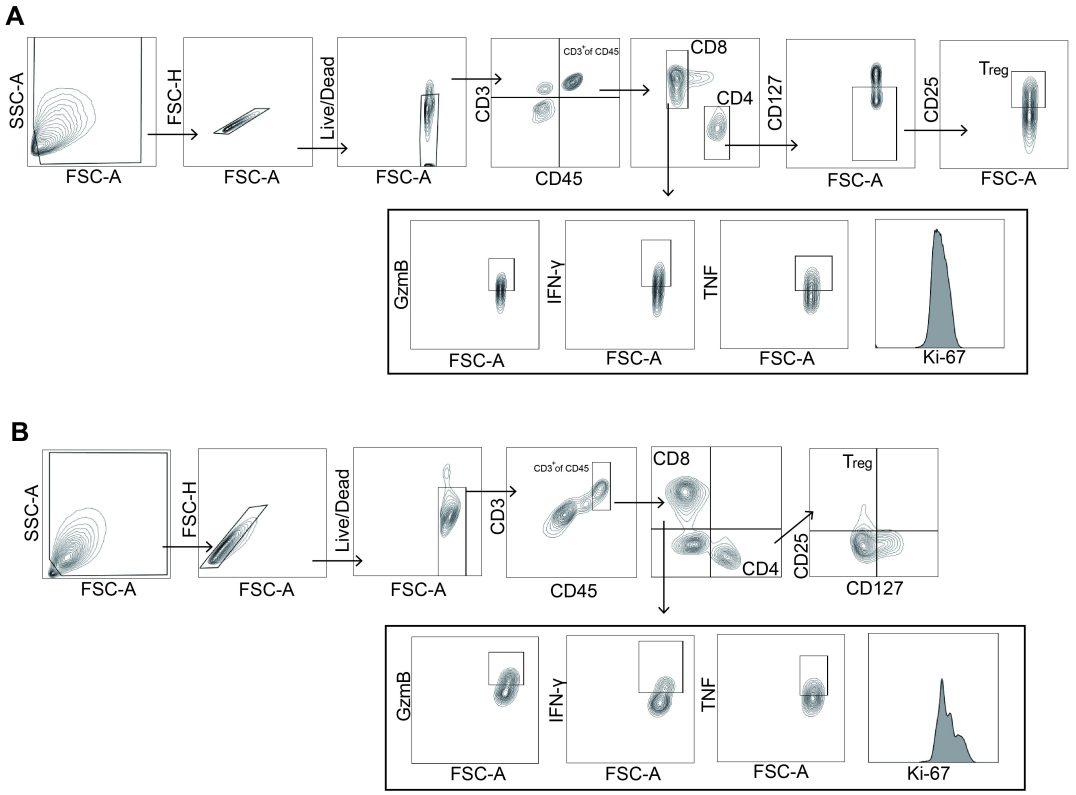

Fig. S10 | Gating strategies used for FACS. (A) Gating strategy to sort CD4, CD8, T_{reg} (CD4+CD127-CD25+), Ki-67 and cytokine production of $CD8^+$ cells from mouse spleen presented on Fig. 7 D-J. (B) Gating strategy to sort CD4, CD8, T_{reg} (CD4+CD127-CD25+), Ki-67 and cytokine production of $CD8^+$ cells from mouse TILs presented on Fig. 7 K-Q.

Supplementary Tables

Table S1 The protein sequence of PD-1^28

MQIPQAPWPVVWAVLQLGWRPGWFLDSPDRPWNPPTFSPALLVVTEGDNATFTCSFSNTSESFVLNW YRMSPSNQTDKLAAFPEDRSQPGQDCRFRVTQLPNGRDFHMSVVRARRNDSGTYLCGAISLAPKAQI KESLRAELRVTGAASEAPGQGEKGRSAHSPPQPLTQASRPVPNPGGWCRGRPAGQPGAASLGPGRH LLPGRTRDNRSQAHRPAPEGGPLSRACVLCGLWGAGFPVAREDPGAPRALCP

206 **Table S2 Nucleotide sequences of *PDCD1^28* (5'-3')**

GGCTCACCTCCGCCTGAGCAGTGGAGAAGGCGGCACTCTGGTGGGGCTGCTCCAGGCATGCAGA
TCCCACAGGCGCCCTGGCCAGTCGTCTGGGCGGTGCTACAACTGGGCTGGCGGCCAGGATGGTT
CTTAGACTCCCCAGACAGGCCCTGGAACCCCCCCACCTTCTCCCCAGCCCTGCTCGTGGTGACCG
AAGGGGACAACGCCACCTTCACCTGCAGCTTCTCCAACACATCGGAGAGCTTCGTGCTAAACTGGT
ACCGCATGAGCCCCAGCAACCAGACGGACAAGCTGGCCGCCTTCCCCGAGGACCGCAGCCAGCC
CGGCCAGGACTGCCGCTTCCGTGTCACACAACTGCCCAACGGGCGTGACTTCCACATGAGCGTGG
TCAGGGCCCGGCGCAATGACAGCGGCACCTACCTCTGTGGGGCCATCTCCCTGGCCCCCAAGGC
GCAGATCAAAGAGAGCCTGCGGGCAGAGCTCAGGGTGACAGGTGCGGCCTCGGAGGCCCCGGG
GCAGGGAGAGAAGGGCAGAAGTGCCCACAGCCCACCCCAGCCCCTCACCCAGGCCAGCCGGCC
AGTTCCAAACCCTGGTGGTTGGTGTCGTGGGCGGCCTGCTGGGCAGCCTGGTGCTGCTAGTCTG
GGTCCTGGCCGTCATCTGCTCCCGGGCCGCACGAGGGACAATAGGAGCCAGGCGCACCGGCCAG
CCCCTGAAGGAGGACCCCTCAGCCGTGCCTGTGTTCTCTGTGGACTATGGGGAGCTGGATTTCCA
GTGGCGAGAGAAGACCCCGGAGCCCCCCGTGCCCTGTGTCCCTGAGCAGACGGAGTATGCCACC
ATTGTCTTTCCTAGCGGAATGGGCACCTCATCCCCCGCCCGCAGGGGCTCAGCTGACGGCCCTCG
GAGTGCCCAGCCACTGAGGCCTGAGGATGGACACTGCTCTTGGCCCCTCTGACCGGCTTCCTTGG
CCACCAGTGTTCTGCAGACCCTCCACCATGAGCCCGGGTCAGCGCATTTCCTCAGGAGAAGCAGG
CAGGGTGCAGGCCATTGCAGGCCGTCCAGGGGCTGAGCTGCCTGGGGGCGACCGGGGCTCCAG
CCTGCACCTGCACCAGGCACAGCCCCACCACAGGACTCATGTCTCAATGCCCACAGTGAGCCCAG
GCAGCAGGTGTCACCGTCCCCTACAGGGAGGGCCAGATGCAGTCACTGCTTCAGGTCCTGCCAG
CACAGAGCTGCCTGCGTCCAGCTCCCTGAATCTCTGCTGCTGCTGCTGCTGCTGCTGCTGCCC
TGCGGCCCGGGGCTGAAGGCGCCGTGGCCCTGCCTGACGCCCCGGAGCCTCCTGCCTGAACTTG
GGGGCTGGTTGGAGATGGCCTTGGAGCAGCCAAGGTGCCCCTGGCAGTGGCATCCCGAAACGCC
CTGGACGCAGGGCCCAAGACTGGGCACAGGAGTGGGAGGTACATGGGGCTGGGGACTCCCCAG
GAGTTATCTGCTCCCTGCAGGCCTAGAGAAGTTTCAGGGAAGGTCAGAAGAGCTCCTGGCTGTGG
TGGGCAGGGCAGGAAACCCCTCCACCTTTACACATGCCCAGGCAGCACCTCAGGCCCTTTGTGGG
GCAGGGAAGCTGAGGCAGTAAGCGGGCAGGCAGAGCTGGAGGCCTTTCAGGCCCAGCCAGCACT
CTGGCCTCCTGCCGCCGCATTCCACCCCAGCCCCTCACACCACTCGGGAGAGGGACATCCTACG
GTCCCAAGGTCAGGAGGGCAGGGCTGGGGTTGACTCAGGCCCCTCCCAGCTGTGGCCACCTGGG
TGTTGGGAGGGCAGAAGTGCAGGCACCTAGGGCCCCCCATGTGCCCACCCTGGGAGCTCTCCTT
GGAACCCATTCCTGAAATTATTTAAAGGGGTTGGCCGGGCTCCCACCAGGGCCTGGGTGGGAAGG
TACAGGCGTTCCCCCGGGGCCTAGTACCCCCGCCGTGGCCTATCCACTCCTCACATCCACACACT
GCACCCCCACTCCTGGGGCAGGGCCACCAGCATCCAGGCGGCCAGCAGGCACCTGAGTGGCTG
GGACAAGGGATCCCCCTTCCCTGTGGTTCTATTATATTATAATTATAATTAAATATGAGAGCATGCT

207

208

Table S3 The name and sequence of ‘other variants’

PD-1Δex2:

ATGCAGATCCCACAGGCGCCCTGGCCAGTCGTCTGGGCGGTGCTACAACTGGGCTGGCGGCCAG
GATGGTTCTTAGAGAGAAGGGCAGAAGTGCCCACAGCCCACCCCAGCCCCTCACCCAGGCCAGC
CGGCCAGTTCCAAACCCTGGTGGTTGGTGTCGTGGGCGGCCTGCTGGGCAGCCTGGTGCTGCTA
GTCTGGGTCCTGGCCGTCATCTGCTCCCGGGCCGCACGAGGGACAATAGGAGCCAGGCGCACCG
GCCAGCCCCTGAAGGAGGACCCCTCAGCCGTGCCTGTGTTCTCTGTGGACTATGGGGAGCTGGAT
TTCCAGTGGCGAGAGAAGACCCCGGAGCCCCCCGTGCCCTGTGTCCCTGAGCAGACGGAGTATG
CCACCATTGTCTTTCCTAGCGGAATGGGCACCTCATCCCCCGCCCGCAGGGGCTCAGCTGACGGC
CCTCGGAGTGCCCAGCCACTGAGGCCTGAGGATGGACACTGCTCTTGGCCCCTCTGA

PD-1Δex3:

ATGCAGATCCCACAGGCGCCCTGGCCAGTCGTCTGGGCGGTGCTACAACTGGGCTGGCGGCCAG
GATGGTTCTTAGACTCCCCAGACAGGCCCTGGAACCCCCCCACCTTCTCCCCAGCCCTGCTCGTG
GTGACCGAAGGGGACAACGCCACCTTCACCTGCAGCTTCTCCAACACATCGGAGAGCTTCGTGCT
AAACTGGTACCGCATGAGCCCCAGCAACCAGACGGACAAGCTGGCCGCCTTCCCCGAGGACCGC
AGCCAGCCCGGCCAGGACTGCCGCTTCCGTGTCACACAACTGCCCAACGGGCGTGACTTCCACAT
GAGCGTGGTCAGGGCCCGGCGCAATGACAGCGGCACCTACCTCTGTGGGGCCATCTCCCTGGCC
CCCAAGGCGCAGATCAAAGAGAGCCTGCGGGCAGAGCTCAGGGTGACAGGGACAATAGGAGCCA
GGCGCACCGGCCAGCCCCTGAAGGAGGACCCCTCAGCCGTGCCTGTGTTCTCTGTGGACTATGG
GGAGCTGGATTTCCAGTGGCGAGAGAAGACCCCGGAGCCCCCCGTGCCCTGTGTCCCTGAGCAG
ACGGAGTATGCCACCATTGTCTTTCCTAGCGGAATGGGCACCTCATCCCCCGCCCGCAGGGGCTC
AGCTGACGGCCCTCGGAGTGCCCAGCCACTGAGGCCTGAGGATGGACACTGCTCTTGGCCCCTC
TGA

PD-1Δex2,3:

ATGCAGATCCCACAGGCGCCCTGGCCAGTCGTCTGGGCGGTGCTACAACTGGGCTGGCGGCCAG
GATGGTTCTTAGGGACAATAGGAGCCAGGCGCACCGGCCAGCCCCTGAAGGAGGACCCCTCAGC
CGTGCCTGTGTTCTCTGTGGACTATGGGGAGCTGGATTTCCAGTGGCGAGAGAAGACCCCGGAGC
CCCCCGTGCCCTGTGTCCCTGAGCAGACGGAGTATGCCACCATTGTCTTTCCTAGCGGAATGGGC
ACCTCATCCCCCGCCCGCAGGGGCTCAGCTGACGGCCCTCGGAGTGCCCAGCCACTGAGGCCTG
AGGATGGACACTGCTCTTGGCCCCTCTGA

PD-1Δex2,3,4:

ATGCAGATCCCACAGGCGCCCTGGCCAGTCGTCTGGGCGGTGCTACAACTGGGCTGGCGGCCAG
GATGGTTCTTAGAAGGAGGACCCCTCAGCCGTGCCTGTGTTCTCTGTGGACTATGGGGAGCTGGA
TTTCCAGTGGCGAGAGAAGACCCCGGAGCCCCCCGTGCCCTGTGTCCCTGAGCAGACGGAGTAT
GCCACCATTGTCTTTCCTAGCGGAATGGGCACCTCATCCCCCGCCCGCAGGGGCTCAGCTGACGG
CCCTCGGAGTGCCCAGCCACTGAGGCCTGAGGATGGACACTGCTCTTGGCCCCTCTGA

209

Table S4 Basic characteristics of patients in this study

Donor	Age	Gender	Samples
Donor1	50-60	Female	lung cancer samples
Donor2	40-50	Female	lung cancer samples
Donor3	60-70	Female	lung cancer samples
Donor4	50-60	Female	lung cancer samples
Donor5	50-60	Male	lung cancer samples
Donor6	60-70	Male	lung cancer samples
Donor7	50-60	Male	lung cancer samples

212 **Table S5 List of RT-PCR, qRT-PCR and RIP qRT-PCR primers**

RT-PCR primers		
Genes	**Forwards (5'-3')**	**Reverses (5'-3')**
PDCD1	AACTGGTACCGCATGAGCCC	TCCAGCTCCCCATAGTCCACAG
qRT-PCR primers		
Genes	**Forwards (5'-3')**	**Reverses (5'-3')**
PDCD1	TCGTGCTAAACTGGTACCGC	TGACCACGCTCATGTGGAAG
GAPDH	GGAGCGAGATCCCTCCAAAAT	GGCTGTTGTCATACTTCTCATGG
CD28	CCCATGCTTGTAGCGTAC	CCCATCACAGTTGAACCC
PDCD1^28	CCCCGGGGCAGGGAGAGAAG	CAGGCACGGCTGAGGGGTCC
PDCD1LG1	GGACAAGCAGTGACCATCAAG	CCCAGAATTACCAAGTGAGTCCT
minigene	GGAGCTCCAGGGTCGTAG	GCTTCCAGAGCTAGAGGACA
TAF15	ACAGCGGTTACTCCAGTTATGG	CCATGTTTTGCTGCTGTCCC
FUS	CAAAGCTATGGGGCCTACCC	ATAGCTGTTCTGGCTCTGGC
EWSR1	TTATGGACAGCCTCCCACTG	TATCCTAGGCTGGGCTGGTT
junction PDCD1	CTTCCACATGAGCGTGGTCA	TGCCCTTCTCTCTGTCACCCT
other variants	ATGCAGATCCCACAGGCG	CTAAGAACCATCCTGGCCGC
RIP qRT-PCR		
Regions	**Forwards (5'-3')**	**Reverses (5'-3')**
PDCD1^28 pre-mRNA	AGGAGCTCCAGGGTCGTAG	GCTTCCAGAGCTAGAGGACA

213

214

Table S6 List of antibodies

Antibodies	Clone	Company	Dilutions
Brilliant Violet 605 anti-mouse CD45	30-F11	biolegend	1:40 for FACS
Alexa Fluor 488 anti-mouse CD3	500A2	biolegend	1:40 for FACS
Brilliant Violet 785 anti-mouse CD4	GK1.5	biolegend	1:40 for FACS
Brilliant Violet 510 anti-mouse CD8	53-6.7	biolegend	1:40 for FACS
Brilliant Violet 421 anti-mouse CD127	A7R34	biolegend	1:40 for FACS
APC-R700 anti-mouse CD25	PC61	BD	1:40 for FACS
PE anti-human/mouse Granzyme B	QA18A28	biolegend	1:100 for FACS
APC/Cyanine7 anti-mouse IFN-γ	XMG1.2	biolegend	1:40 for FACS
PerCP/Cyanine5.5 anti-mouse TNF	MP6-XT22	biolegend	1:40 for FACS
APC anti-mouse Ki-67	16A8	biolegend	1:40 for FACS
PE anti-mouse/human CD44	IM7	biolegend	1:40 for FACS
APC/Cyanine7 anti-mouse CD62L	MEL-14	biolegend	1:40 for FACS
APC-R700 anti-human CD45	HI30	BD	1:40 for FACS
Alexa Fluor 488 anti-human CD3	UCHT1	BD	1:40 for FACS
BV650 anti-human CD4	SK3	BD	1:40 for FACS
Brilliant Violet 785 anti-human CD8	SK1	biolegend	1:40 for FACS
Brilliant Violet 421 anti-human CD127	A019D5	biolegend	1:40 for FACS
PE anti-human CD25	BC96	biolegend	1:40 for FACS
Alexa Fluor 647 anti-human/mouse Granzyme B	GB11	biolegend	1:40 for FACS
FITC anti-human IFN-γ	4S.B3	biolegend	1:40 for FACS
Alexa Fluor 700 anti-human TNF	MAb11	biolegend	1:40 for FACS
Brilliant Violet 510 anti-human Ki-67	Ki-67	biolegend	1:40 for FACS
APC anti-human CD279	MIH4	BD	1:40 for FACS
Brilliant Violet 421 anti-human CD4	RPA-T4	biolegend	1:40 for FACS
PD-1 monoclonal antibody	OTI21F5	OriGene	1:1000 for WB
PD-L1 monoclonal antibody	E1L3N	CST	1:1000 for WB
GAPDH monoclonal antibody	1E6D9	proteintech	1:2000 for WB

215

216 **Table S7 Antigen sequence for PD-1^28 antibodies**

GAASEAPGQGEKGRSAHSPPQPLTQASRPVPNPGGWCRGRPAGQPGAASLGPGRHLLPGRTRDNR SQAHRPAPEGGPLSRACVLCGLWGAGFPVAREDPGAPRALCP

217

218

Table S8 Sequences of shRNA for KD

Targets	shRNA-Forward (5'-3')	shRNA-Reverse (5'-3')
sh-PDCD1^28-1	GATCCGGGAGAGAAGGGCAGAAGTGCTTCAAGAGAGCACTTCTGCCCTTCTCTCCCTTTTTTG	AATTCAAAAAAGGGAGAGAAGGGCAGAAGTGCTCTCTTGAAGCACTTCTGCCCTTCTCTCCCG
sh- PDCD1^28-2	GATCCGGGCAGGGAGAGAAGGGCAGATTCAAGAGATCTGCCCTTCTCTCCCTGCCCTTTTTTG	AATTCAAAAAAGGGCAGGGAGAGAAGGGCAGATCTCTTGAATCTGCCCTTCTCTCCCTGCCCG
sh-TAF15-1	GATCCGGACAGAACTACAGCGGTTACTTCAAGAGAGTAACCGCTGTAGTTCTGTCCTTTTTTG	AATTCAAAAAAGGACAGAACTACAGCGGTTACTCTCTTGAAGTAACCGCTGTAGTTCTGTCCG
sh- TAF15-2	GATCCGCCACTAGAAGACCTGAATTCTTCAAGAGAGAATTCAGGTCTTCTAGTGGCTTTTTTG	AATTCAAAAAAGCCACTAGAAGACCTGAATTCTCTCTTGAAGAATTCAGGTCTTCTAGTGGCG
sh-FUS-1	GATCCGCAGAGTTACAGTGGTTATAGTTCAAGAGACTATAACCACTGTAACTCTGCTTTTTTG	AATTCAAAAAAGCAGAGTTACAGTGGTTATAGTCTCTTGAACTATAACCACTGTAACTCTGCG
sh-FUS-2	GATCCGGGTGAGAATGTTACAATTGATTCAAGAGATCAATTGTAACATTCTCACCCTTTTTTG	AATTCAAAAAAGGGTGAGAATGTTACAATTGATCTCTTGAATCAATTGTAACATTCTCACCCG
sh-EWSR1-1	GATCCGCCAAGCTCCAAGTCAATATATTCAAGAGATATATTGACTTGGAGCTTGGCTTTTTTG	AATTCAAAAAAGCCAAGCTCCAAGTCAATATATCTCTTGAATATATTGACTTGGAGCTTGGCG
sh-EWSR1-2	GATCCGGCAACCCATGATCCACATCTTTCAAGAGAAGATGTGGATCATGGGTTGCCTTTTTTG	AATTCAAAAAAGGCAACCCATGATCCACATCTTCTCTTGAAAGATGTGGATCATGGGTTGCCG

219